Water Supply

IWA PUBLISHING

Water Supply Vol 22 No 1, 452 doi: 10.2166/ws.2021.262

Changes in soil-water content and heat transport under different simulated systems of drip irrigation in gravel-mulched fields

Wenju Zhao [a,*], Yali Wang [a], Junhong Hu[a], Zongli Li[a], Yingdong Zhao[b] and Guihua Qi[b]

[a] College of Energy and Power Engineering, Lanzhou University of Technology, Lanzhou 730050, China
[b] Water Resources Utilization Center of Taolai River Basin, Water Resources Department of Gansu Province, Jiuquan 735000, China
*Corresponding author. E-mail: wenjuzhao@126.com

WZ, 0000-0001-6204-1842; YW, 0000-0002-6545-7808

ABSTRACT

Gravel mulching is an ancient mulching system with a history of more than 300 years in China. To explore the changes of soil-water content (SWC) and heat transport in watermelon gravel-mulched fields under drip irrigation, we simulated three irrigation quotas (W1, 180 m^3/hm^2; W2, 270 m^3/hm^2; and W3, 360 m^3/hm^2) and three irrigation frequencies (F1, three times; F2, six times; and F3, nine times) based on HYDRUS-2D. The results indicated that peak SWC increased with irrigation quota. The range of fluctuation of SWC decreased as irrigation frequency increased. The temperature of the 0–40 cm soil layer varied with air temperature, but the range of fluctuation decreased with depth. Irrigation affected the distribution of soil water, increased soil heat capacity, and reduced the impact of air temperature on soil temperature, thus delaying the impact of air temperature on soil temperature. High-frequency drip irrigation could therefore effectively improve SWC, reduce water stress during the period of watermelon growth, and effectively delay the effect of air temperature on soil temperature, providing a theoretical basis for developing reasonable irrigation strategies and regulating soil water and heat in gravel-mulched fields.

Key words: gravel mulched field, irrigation frequency, irrigation quotas, numerical simulation, water and heat distribution

HIGHLIGHTS

- Irrigation affects the distribution of soil moisture and the change of soil temperature.
- Under the same irrigation quota, a high-frequency irrigation system is beneficial for increasing the water content of the soil.
- High-frequency drip irrigation can effectively reduce the impact of air temperature on the temperature of the soil cultivated layer.

INTRODUCTION

The conditions of soil water and heat are important ecological environmental factors that affect the growth and development of crops and are directly associated with farming methods. Reasonable farming methods (such as mulching and irrigation) can create suitable environments of water and heat for crop growth and development, which are key measures for sustained high crop yields (Dong *et al.* 2014; Yang *et al.* 2018). Gravel-mulching is an ancient mulching system with a history of more than 300 years in China. Sand and gravel mulches on the soil surface can increase the rate of use of precipitation, inhibit soil evaporation, prevent secondary salinization, improve soil physical and chemical properties, and substantially increase the storage of water in the soil. Gravel mulching can also conserve soil heat and ultimately increase crop yield (Wang *et al.* 2017; Zhao *et al.* 2017, 2019, 2020). Gravel mulching is used in rain-fed agriculture, but rainfall often cannot meet the water demand during crop growth, thereby decreasing yields. Supplementary irrigation is therefore particularly necessary for gravel-mulched fields. Xie *et al.* (2006) proposed that drip irrigation should replace the previously used extensive flood irrigation. Drip irrigation can increase crop yields in gravel-mulched fields and can stabilize and increase output without aggravating the degradation of gravel-mulched fields.

As a local water-saving method of irrigation applied near the root zones of crops, drip irrigation can be used for managing water and fertilizer use at any time based on the conditions of crop growth. It is widely used in practices of agricultural production and has substantial advantages for conserving water and increasing yields. Different volumes and frequencies of

irrigation, however, will inevitably have different effects on crop growth and the distribution and migration of soil water and heat (Sui *et al.* 2008). Irrigation frequency with the same amount of water is one of the most important factors affecting the conditions of soil water and heat, the use efficiencies of water and fertilizer, and crop yield (Jha *et al.* 2017; Liu *et al.* 2019). Chastain *et al.* (2015) reported that repeated irrigation can greatly increase the yield of ryegrass seed compared with a single irrigation. Cao *et al.* (2003) found that irrigation frequency could affect the spatial distribution of soil water and the capacity of soil to store water and that an appropriate irrigation frequency in indoor homogeneous soil-column experiments could increase the total volume of water stored in the soil. Wang *et al.* (2008) found that the average soil-water content (SWC) with high-frequency drip irrigation fluctuated within a relatively stable small range and that drip irrigation could substantially delay the impact of air temperature on ground temperature.

Understanding soil water and temperature is important for the management of drip irrigation, farming, and fertilization. Most studies have investigated the transport of soil water and heat under conditions of plastic-mulching and irrigation using numerical simulations (He *et al.* 2018; Zhao *et al.* 2018b; Grecco *et al.* 2019). Zhang *et al.* (2018) reported that the HYDRUS model could well simulate SWC and heat transfer for potato farmland under drip irrigation with film mulching. Many studies of gravel-mulched fields have mainly focused on changes in SWC (Wang *et al.* 2018; Zhao *et al.* 2020), salt transport (Tan *et al.* 2018; Hu *et al.* 2020), the impact of irrigation systems on crop yields (Ma & Tian 2016), and the effect of evaporation on gravel-mulched fields (Yuan *et al.* 2009; Ma & Li 2011). The impacts of different drip-irrigation systems on SWC and heat transfer in gravel-mulched fields, however, have not yet been studied. We therefore used HYDRUS-2D to simulate changes in SWC and heat in gravel-mulched soil under different irrigation quotas and frequencies, determine the influence of the drip-irrigation systems on the distribution of soil water and heat in a gravel-mulched field, and identify the mechanisms of changes to SWC and heat in a gravel-mulched field under drip irrigation. This study provides theoretical guidance for the design of a reasonable irrigation system for watermelon gravel-mulched fields and for the rational regulation of soil water and heat in these fields.

NUMERICAL MODEL

HYDRUS-2D is a popular software that can simulate water, heat and nutrient dynamics in variably saturated porous media (Šimůnek *et al.* 2016). HYDRUS-2D uses the Galerkin finite-element method to solve the Richards equations of saturated and unsaturated water flows and the convection–dispersion equations of heat and solute transport. Our study used watermelon on gravel-mulch as the research object, with three drip-irrigation quotas (W1, 180 m^3/hm^2; W2, 270 m^3/hm^2; and W3, 360 m^3/hm^2) and three irrigation frequencies (F1, three times; F2, six times; and F3, nine times), for a total of nine treatments (Table 1). The simulated period was from 31 May to 11 August 2019, for a total of 72 d. The optimal irrigation volume was determined based on the upper and lower limits of SWC. The upper SWC limit was the water-holding capacity of the field (24% SWC by weight) (Ma & Tian 2016), and the lower SWC limit was the most suitable amount of water for each stage of watermelon growth: 40% water-holding capacity at the seedling stage, 50% water-holding capacity at the vining

Table 1 | Irrigation treatments of watermelon in growth period in gravel-mulched field

			Irrigation amount at each data (m^3/hm^2)								
Treatment	**Irrigation quota (m^3/hm^2)**	**Irrigation frequency**	**06–01**	**06–08**	**06–15**	**06–25**	**07–01**	**07–10**	**07–17**	**07–25**	**08–05**
W1F1	180	3	60	0	0	60	0	0	0	60	0
W1F2	180	6	30	0	30	30	0	30	0	30	30
W1F3	180	9	20	20	20	20	20	20	20	20	20
W2F1	270	3	90	0	0	90	0	0	0	90	0
W2F2	270	6	45	0	45	45	0	45	0	45	45
W2F3	270	9	30	30	30	30	30	30	30	30	30
W3F1	360	3	120	0	0	120	0	0	0	120	0
W3F2	360	6	60	0	60	60	0	60	0	60	60
W3F3	360	9	40	40	40	40	40	40	40	40	40

stage, 40% water-holding capacity at the flowering and fruiting stages, 60% water-holding capacity at the swelling stage, and 50% water-holding capacity at the maturation stage.

Numerical modeling theory for soil water flow

Assuming that the soil in each layer is a homogeneous, isotropic, and nondeformable porous medium, and assuming that the flow of soil water is axisymmetric under point-source drip irrigation, the flow of water can be simplified as an axisymmetric two-dimensional problem. The flow of soil water is simulated by (Šimůnek *et al.* 1999):

$$\frac{\partial \theta}{\partial t} = \frac{\partial}{\partial r}\left[K(h)\frac{\partial h}{\partial r}\right] + \frac{\partial}{\partial z}\left[K(h)\left(\frac{\partial h}{\partial z} - 1\right)\right] - S(h) \tag{1}$$

where r is the radial coordinate, cm; z is the vertical coordinate, cm; θ is volumetric SWC, cm^3/cm^3; h is the matrix potential, cm; t is time, d; $K(h)$ is the unsaturated hydraulic conductivity of the soil, cm/d; and $S(h)$ is the amount of water absorbed by roots, cm/d.

The unsaturated soil water characteristic curve θ and soil unsaturated hydraulic conductivity $K(h)$ are represented by the van Genuchten model (van Genuchten 1980) in HYDRUS-2D simulation, without considering the hysteretic effect:

$$\theta(h) = \theta_r + \frac{\theta_s - \theta_r}{(1 + |\alpha h|^n)^m} \quad h < 0 \tag{2}$$

$$\theta(h) = \theta_s \quad h > 0 \tag{3}$$

$$K(h) = K_s S_e^l [1 - (1 - S_e^{l/m})^m]^2 \tag{4}$$

where $S_e = (\theta - \theta_r)(\theta_s - \theta_r)$ and $m = 1 - 1/n$; θ_r is residual SWC, cm^3/cm^3; θ_s is saturated SWC, cm^3/cm^3; K_s is saturated soil hydraulic conductivity, cm/d; α, m, and n are fitting parameters; and $l = 0.5$.

Numerical modeling theory for heat transport

Ignoring the diffusion of vapor water and considering only the influence of the flow of liquid water on the transfer of soil heat, the two-dimensional soil heat flow motion control is calculated as (Šimůnek *et al.* 1999):

$$C(\theta)\frac{\partial T}{\partial t} = \frac{\partial}{\partial r}(\lambda_{ij}\frac{\partial T}{\partial z}) - C_w q_i \frac{\partial T}{\partial r} \tag{5}$$

where $C(\theta)$ is the specific heat capacity of the porous medium, J/(g·°C); C_w is the specific heat capacity of the liquid, J/(g·°C); λ_{ij} is soil thermal conductivity, J/(cm·°C); q_i is water flux, cm; T is soil temperature, °C; r is the radial coordinate, cm; and z is the vertical coordinate, cm.

Root water absorption

The authors used the Feddes model for calculating the absorption of water by roots:

$$S(x, z, h) = \alpha(x, z, h)b(x, z)LT_p \tag{6}$$

where $\alpha(x, z, h)$ is the stress coefficient; $b(x, z)$ is the standardized function for root distribution; L is maximum root width, cm; and T_p is potential transpiration, cm/d. The root-distribution function is determined by (Vrugt *et al.* 2001):

$$b(x, z) = \left(1 - \frac{z}{Z_m}\right)\left(1 - \frac{x}{X_m}\right)e^{-\left(\frac{P_z}{Z_m}|z^* - z| + \frac{P_x}{X_m}|x^* - x|\right)} \tag{7}$$

where X_m is the maximum length of the distribution of roots in the horizontal direction; Z_m is the maximum length of the distribution of roots in the vertical direction; x^* is maximum root density in the horizontal direction; z^* is maximum root density in the vertical direction; and P_x and P_z are parameters of the symmetry of the root system in the horizontal and vertical directions, respectively.

Initial conditions

In the calculation domain of the HYDRUS-2D model, assuming that the initial SWC and soil temperature are uniformly distributed throughout the profile, the initial conditions of SWC and temperature are:

$$\theta_i(r, z, t) = \theta_{0i}(r, z, 0); 0 \le r \le 50\,\text{cm}, 0 \le z \le 110\,\text{cm} \quad t = 0 \tag{8}$$

$$T_i(r, z, t) = T_{0i}(r, z, 0); 0 \le r \le 50\,\text{cm}, 0 \le z \le 110\,\text{cm} \quad t = 0 \tag{9}$$

where $\theta_{0i}(r, z, 0)$ is the initial SWC, cm^3/cm^3; and $T_{0i}(r, z, 0)$ is the initial soil temperature, °C.

Boundary conditions

The simulated area was a rectangle with a length (vertical) of 100 cm and a width (horizontal) of 50 cm. The soil texture in the simulated area was assumed to be uniform and isotropic. The upper boundary of the saturated area for calculation was the flux boundary that varied over time during drip irrigation, which was the third type of boundary condition, and the temperature boundary condition was the third type of boundary condition (Cauchy boundary). Without irrigation, the upper boundary was the atmospheric boundary. The temperature boundary condition was the first type of boundary condition (Dirichlet boundary). The left and right boundaries of the simulated area for calculation were assumed to be impervious, i.e. were zero-flux boundaries, and the temperature boundary condition was the second type of boundary condition (Neumann boundary). The lower boundary of the simulated area for calculation was assumed to be a free-drainage boundary condition due to the depth of the groundwater. The flow boundary condition was then the first type of boundary condition, and the temperature boundary condition was the second type of boundary condition (Neumann boundary).

Model parameters

The thickness of the gravel layer in the simulated area was 10 cm, the soil depth was 100 cm, and the parameters of soil-water transport were predicted using neural networks and the Rosetta module in HYDRUS, based on the composition of the soil particles (part of the American agricultural system). The soil hydraulic parameters are presented in Table 2, and the parameters for the transfer of heat in the soil are presented in Table 3.

RESULTS AND DISCUSSION

Dynamic changes in SWC

SWC of each layer in the nine irrigation treatments tended to increase during irrigation and then gradually decreased as the water evaporated (Figure 1). Under the same irrigation volume, due to the large single irrigation volume, the peak SWC of low-frequency irrigation is larger than that of medium-frequency and high-frequency. For example, the maximum peak SWC of the 10–40 cm layer treated by W1F1 is 2.09%–7.62% and 2.28%–12.08% higher than those of W1F2 and W1F3,

Table 2 | Soil hydraulic parameters

Type	Depth/cm	θ_r/cm³·cm⁻³	θ_s/cm³·cm⁻³	α/cm⁻¹	n	K_s/cm.d⁻¹
Sand	0–10	0.0544	0.384	0.0302	4.705	1,567.1
Sandy Loam	10–110	0.0352	0.382	0.0052	1.587	112.4

Table 3 | Soil thermal transfer parameters

Type	Solid	Org	D_L	D_T	b_1	b_2	b_3	C_n	C_o	C_w
Sand	0.57	0	5	1	4.92×10^6	-5.20×10^7	10.6×10^8	6.91×10^7	9.04×10^7	1.50×10^8
Sandy Loam	0.59	0	5	1	5.25×10^6	8.49×10^6	3.31×10^7	6.91×10^7	9.04×10^7	1.50×10^8

Note: Solid is the ratio of soil solid to total volume; Org is the ratio of organic matter to total volume; D_L is the longitudinal thermal diffusivity ($cm^2 \cdot s^{-1}$); D_T is the transverse thermal diffusivity ($cm^2 \cdot s^{-1}$); b_1, b_2 and b_3 are the coefficients in the thermal conductivity function; C_n, C_o and C_w are the heat capacity of soil solid phase, soil organic matter and soil liquid phase ($J \cdot g^{-1} \cdot °C^{-1}$).

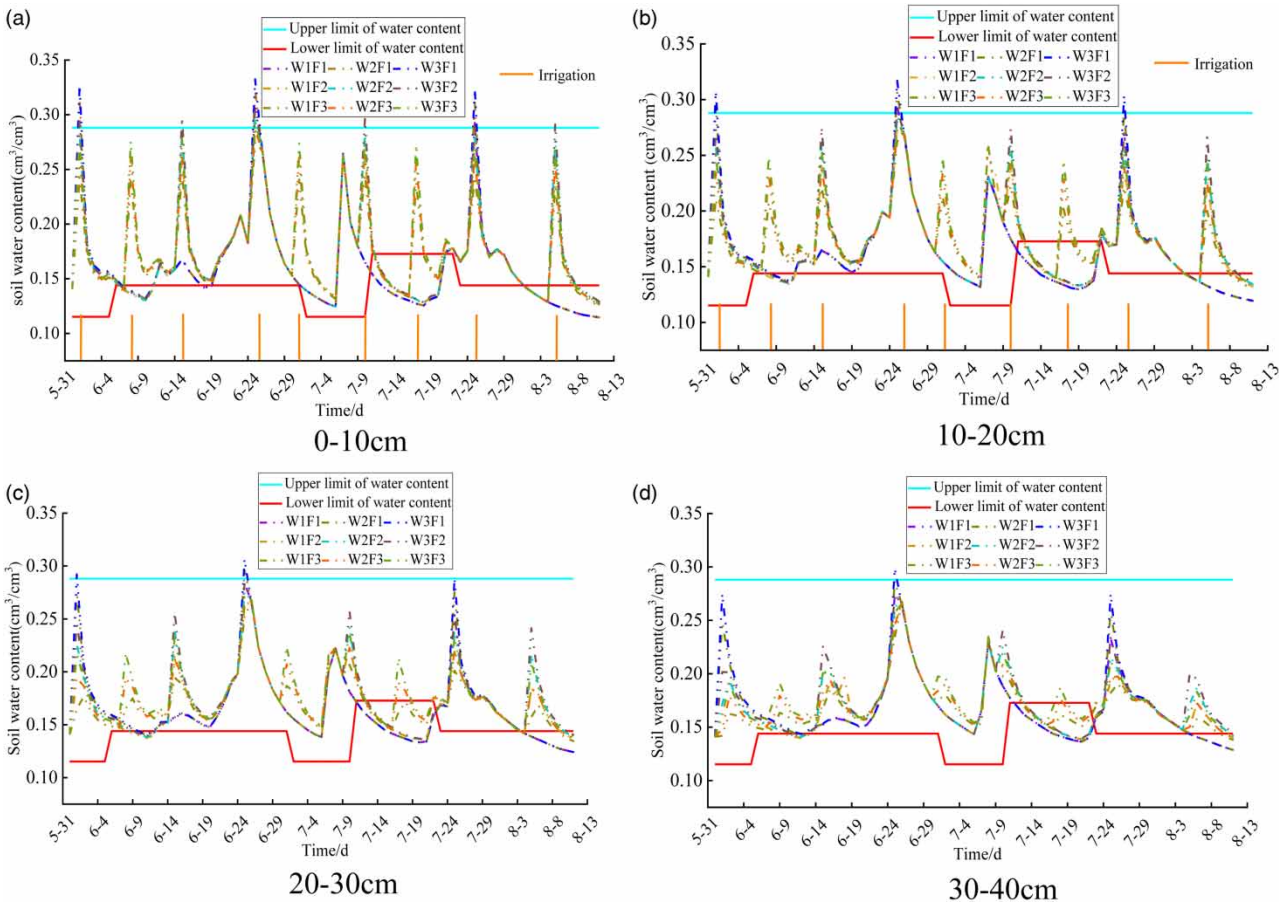

Figure 1 | Dynamic change in soil-water content in the 0–40 cm layer under the irrigation treatments.

respectively. But with the increase of irrigation frequency, the fluctuation range of SWC decreases. High-frequency irrigation has the characteristics of 'less irrigation for many times', which makes the SWC of the wet layer higher than other treatments, which is consistent with the research conclusion of Sui *et al.* (2008).

SWC was within the upper limit for all three irrigation quotas, but SWC for F1 was lower than the water content required at the later stages of watermelon growth (Figure 1). The lower limit is when the watermelon will be under some amount of water stress. High-frequency irrigation can effectively reduce the duration of water stress during growth and ensure enough water for growth. Cao *et al.* (2003) found that increasing irrigation frequency, if appropriate, for the same total irrigation volume could play a role in increasing the amount of soil water stored. Zhang *et al.* (2020) also found that volumetric SWC was higher under high-frequency irrigation than conventional frequency. The amplitude of fluctuation of SWC was smaller for F3 than the other treatments, indicating that high-frequency irrigation could maintain SWC within a relatively stable range, consistent with the conclusions of Wang *et al.* (2008).

Distribution of water in the soil profile

An appropriate irrigation volume has a large impact on improving the efficiency of use of soil water. At the same irrigation volume, the higher the frequency, the smaller the volume of a single irrigation and the shallower the depth of water infiltration. Taking the W1 irrigation quotas as an example, the water distribution of the soil profile after irrigation with different treatments is analyzed. The depth of water infiltration at the end of irrigation was >50, 45, and 40 cm for W1F1, W1F2, and W1F3, respectively (Figure 2). The depth of water infiltration was in the order W1F1 > W1F2 > W1F3, and the moist range reached a reasonable water-absorbing root system area of the watermelon. The volumetric SWC of the soil surrounding the drippers gradually decreased 1–2 d after irrigation, and the body of wet soil continued to move downward. The migration distance of the wet soil body was in the order W1F1 > W1F2 > W1F3. Excessive irrigation could thus easily cause the deep

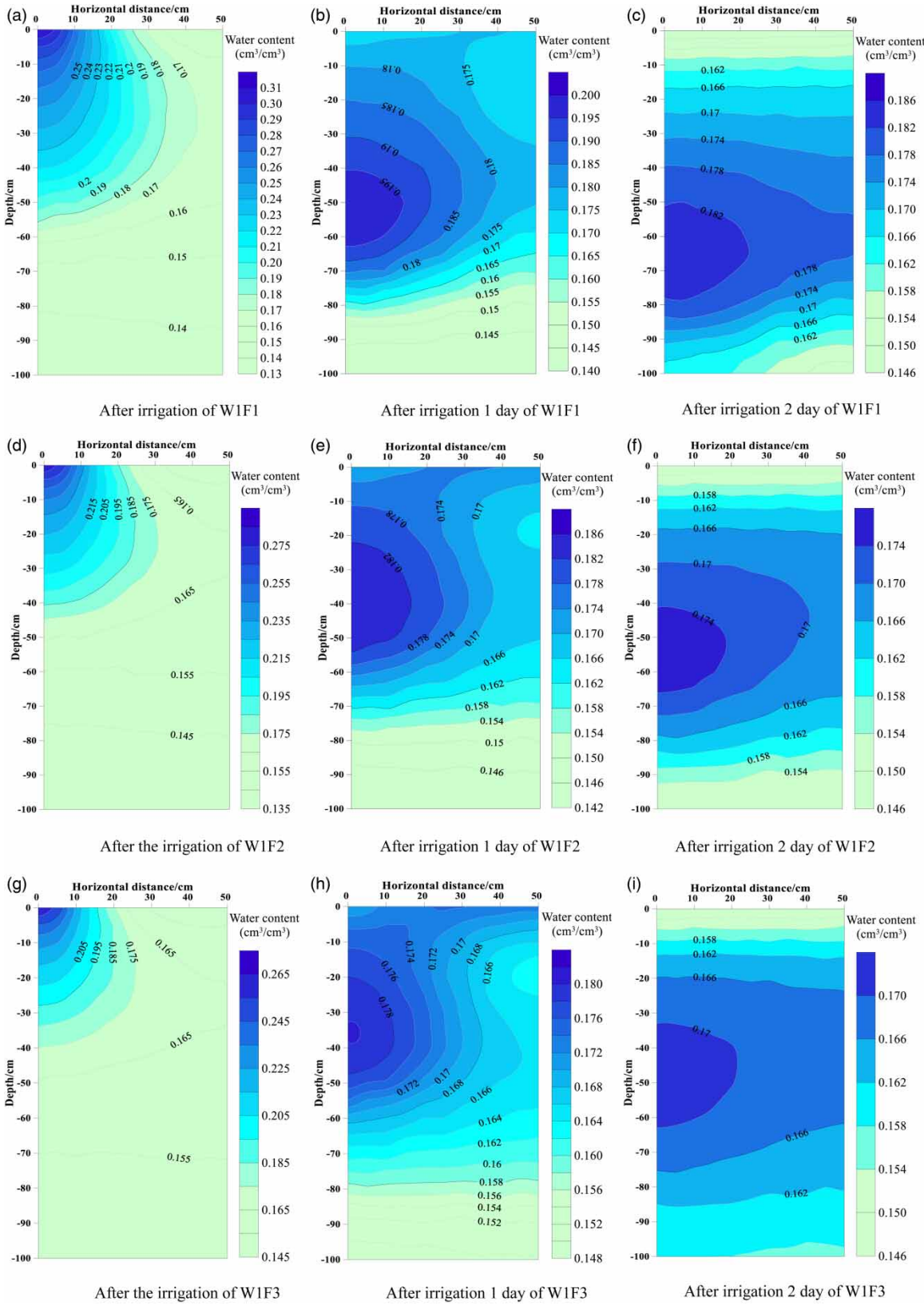

Figure 2 | Distribution of water in the soil profile after irrigation of W1F1 (a–c), W1F2 (d–f) and W1F3 (g–i).

infiltration of water that cannot be effectively used by the root system. Increasing the frequency of irrigation to reduce the volume of single irrigations could therefore increase SWC in the main root zone and increase the water-use efficiency of the plant.

Dynamics of soil temperature

Solar radiation is the main source of heat for soil. Heat is continuously exchanged between the soil and the atmosphere everywhere. The amount of heat in the soil will also vary due to changes in SWC, thereby affecting the distribution of soil temperature. The trend of change of soil temperature was similar among the irrigation treatments in our study (Figure 3). The temperature of each layer varied with the air temperature. The temperature of the surface layer (0–10 cm) was strongly affected by the air temperature, and the temperature fluctuated greatly with the changes in air temperature. The fluctuations in soil temperature were mainly correlated with air temperature, irrigation, and rainfall. The deeper the soil layer, the smaller the influence of air temperature, irrigation, and rainfall, and the smaller the range of fluctuation. The range of fluctuation of the soil temperature decreased with depth, consistent with the results reported by Zhao *et al.* (2018a).

Differences in SWC are a key factor that determines how fast the soil temperature fluctuates due to changes in air temperature. The soil temperature in our study tended to decrease after irrigation, and the increase in temperature decreased, because SWC increased after irrigation and the specific heat capacity of the soil increased with SWC. Irrigation generally delayed the impact of air temperature on soil temperature, because irrigation affected the distribution of water and increased the specific heat capacity of the soil.

Distribution of temperature in the soil profile

The change of soil temperature is closely related to the law of soil water movement. It can be seen from Figure 4 that after irrigation, the soil temperature distribution of the W1F1–W1F3 treatments showed a trend of change from high to low in the

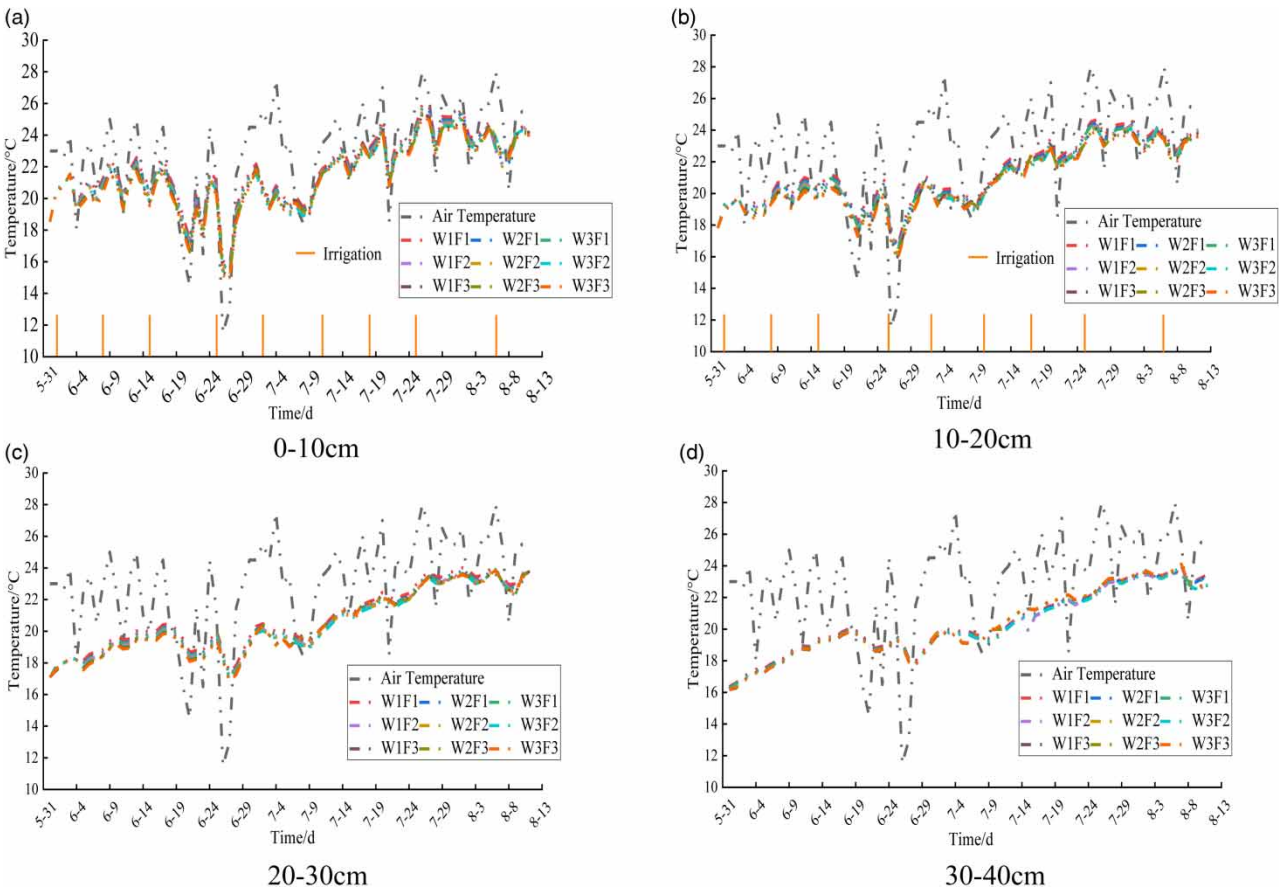

Figure 3 | Dynamic changes in soil temperature in the 0–40 cm layer under the irrigation.

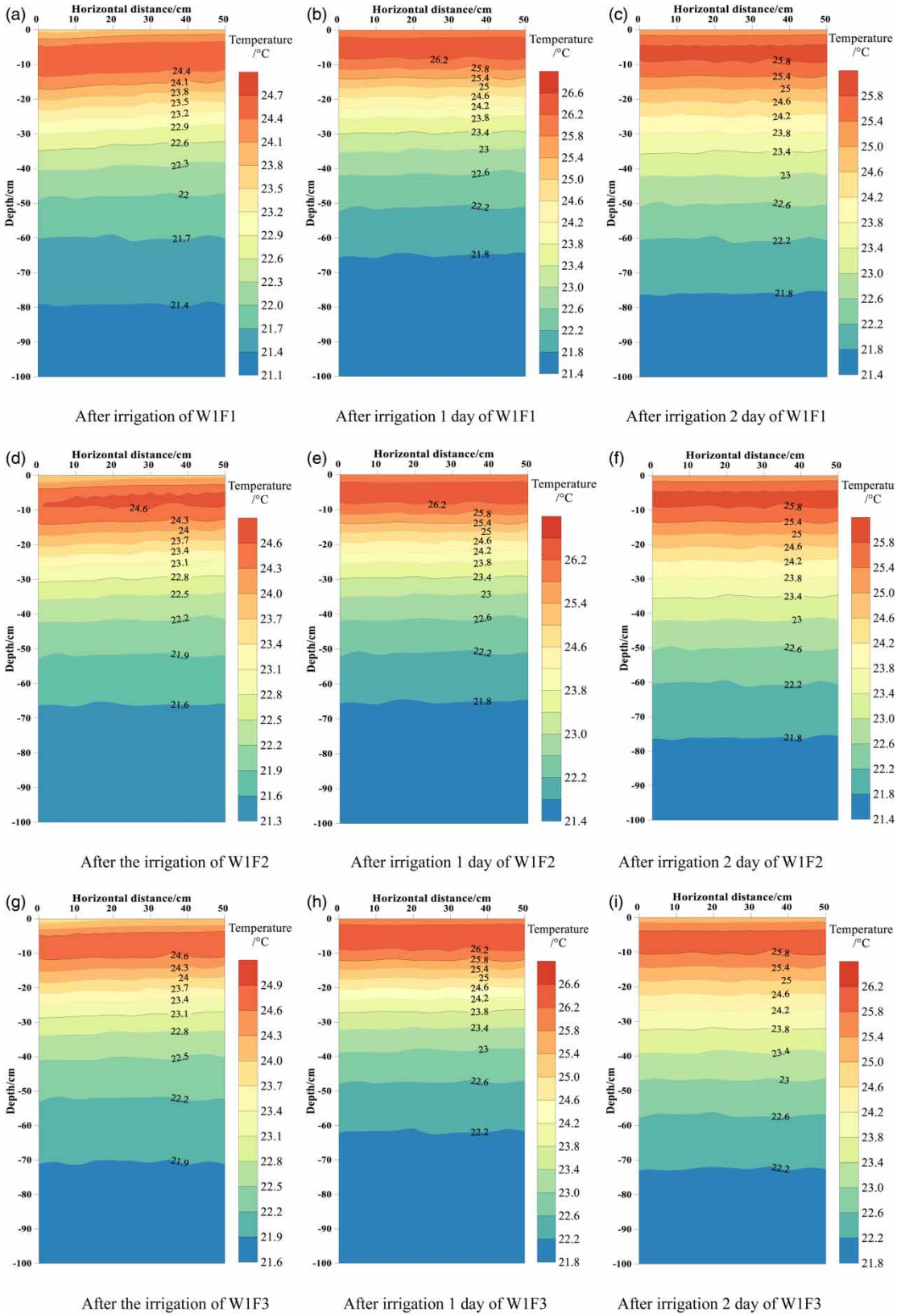

Figure 4 | Temperature distribution of soil profile after irrigation of W1F1 (a–c), W1F2 (d–f) and W1F3 (g–i).

vertical direction. The temperature of the soil surface 0–30 cm of the three treatments is 0.5–2.0 °C lower than that of one day after irrigation. This is because after irrigation, the soil temperature decreases with the increase of soil moisture content, indicating that irrigation has a cooling effect on the soil. The surface soil temperature has the largest variation range, while the deep soil is less affected by irrigation, indicating that the influence of irrigation on the surface soil temperature is greater than that of the deep soil. With the influence of soil water consumption and air temperature, the soil temperature increases. This is because the soil temperature drops after irrigation. After the irrigation is completed, the soil temperature slowly rises as the soil moisture is consumed. This is consistent with the results of Qi *et al.* (2019).

CONCLUSIONS

Irrigation quotas and frequency strongly affected the distribution of soil water. Irrigation quotas affected SWC by increasing peak SWC as irrigation volume increased. Irrigation frequency affected SWC by decreasing the range of fluctuation of SWC as irrigation frequency increased. The range of fluctuation of SWC was smaller for F3 than for F1 and F2, which is conducive to maintaining SWC within a relatively stable range and effectively reducing the duration of water stress during the period of watermelon growth. The changes in soil temperature tended to be similar in all irrigation treatments. The temperature of each soil layer varied with the changes in air temperature. The temperature of the surface soil layer (0–10 cm) was greatly affected by the air temperature, with large fluctuations with changes in air temperature. The range of fluctuation of soil temperature decreased with depth. Our comprehensive analysis of the effects of different drip-irrigation systems on the distribution of soil water and heat in compacted gravel-mulched soil indicated that high-frequency drip irrigation at the same irrigation volume was conducive to maintaining SWC within a relatively stable range, increasing SWC of the cultivated layer, and effectively regulating changes in soil temperature.

ACKNOWLEDGEMENTS

This research was supported by National Natural Science Foundation of China (51869010), Guidance Program for Industrial Support of Colleges and Universities in Gansu Province (2019C-13), Longyuan Youth Innovation and Entrepreneurship Project and the Lanzhou University of Technology Hongliu first-class discipline funding and Water Conservancy Science Experimental Research and Technology Extension Project of Gansu Province.

DATA AVAILABILITY STATEMENT

All relevant data are included in the paper or its Supplementary Information.

REFERENCES

Cao, H. X., Kang, S. Z. & He, H. 2003 Effects of evaporation and irrigation frequency on soil water distribution. *Transactions of the Chinese Society of Agricultural Engineering* **19** (6), 1–4.

Chastain, T. G., King, C. M., Garbacik, C. J., Young, W. C. & Wysocki, D. J. 2015 Irrigation frequency and seasonal timing effects on perennial ryegrass (*Lolium perenne* L.) seed production. *Field Crops Research* **180**, 126–134.

Dong, B., Liu, M., Jiang, J., Shi, C., Wang, X., Qiao, Y., Liu, Y., Zhao, Z., Li, D. & Si, F. 2014 Growth, grain yield, and water use efficiency of rain-fed spring hybrid millet (*Setaria italica*) in plastic-mulched and unmulched fields. *Agricultural Water Management* **143**, 93–101.

Grecco, K. L., de Miranda, J. H., Silveira, L. K. & van Genuchten, M. T. 2019 HYDRUS-2D simulations of water and potassium movement in drip irrigated tropical soil container cultivated with sugarcane. *Agricultural Water Management* **221**, 334–347.

He, Q., Li, S., Kang, S., Yang, H. & Qin, S. 2018 Simulation of water balance in a maize field under film-mulching drip irrigation. *Agricultural Water Management* **210**, 252–260.

Hu, J. H., Zhao, W. J., Liu, G. Y. & Hu, J. Z. 2020 Numerical simulation of the influence of water and soil temperature on water and heat transfer of sand mulching soil under drip irrigation. *Journal of Soil and Water Conservation* **34** (5), 349–354 & 360.

Jha, S. K., Gao, Y. & Liu, H. 2017 Root development and water uptake in winter wheat under different irrigation methods and scheduling for North China. *Agricultural Water Management* **182**, 139–150.

Liu, H., Li, H., Ning, H., Zhang, X., Li, S., Peng, J., Wang, G. & Sun, J. 2019 Optimizing irrigation frequency and amount to balance yield, fruit quality and water use efficiency of greenhouse tomato. *Agricultural Water Management* **226**, 105787.

Ma, Y. J. & Li, X. Y. 2011 Water accumulation in soil by gravel and sand mulches: influence of textural composition and thickness of mulch layers. *Journal of Arid Environments* **75** (5), 432–437.

Ma, B. & Tian, J. C. 2016 Research on the optimal irrigation schedule of watermelon in gravel mulch field based on Jensen model. *Agricultural Research in the Arid Areas* **34** (6), 123–129 & 155.

Qi, Y. L., Shi, H. B., Li, R. P., Zhao, J., Li, B. & Li, M. 2019 Effects of film mulching on maize growth and soil water, fertilizer and heat under fertigation of drip irrigation. *Transactions of the Chinese Society of Agricultural Engineering* **35** (5), 99–110.

Šimůnek, J., Šejna, M. & van Genuchten, M. T. 1999 *The HYDRUS-2D Software Package for Simulating the Two Dimensional Movement of Water, Heat and Multiple Solutes in Variably-Saturated Media*. US Salinity Laboratory, Riverside, CA, USA.

Šimůnek, J., van Genuchten, M. T. & Šejna, M. 2016 Recent developments and applications of the HYDRUS computer software packages. *Vadose Zone Journal* **15** (7), 1–25.

Sui, J., Gong, S. H., Wang, J. D., Zou, H. & Yu, Y. D. 2008 Effects of drip irrigation frequency on the distribution of soil water, soil temperature and maize grown in north China. *Journal of Soil and Water Conservation* **22** (4), 148–152.

Tan, J. L., Wang, X. N., Tian, J. C. & SU, X. L. 2018 Effect of gravel–sand mulching on movements of soil water and salts under different amounts of brackish water. *Transactions of the Chinese Society of Agricultural Engineering* **34** (17), 100–108.

van Genuchten, M. T. 1980 A closed-form equation for predicting the hydraulic conductivity of unsaturated soils. *Soil Science Society of America Journal* **44** (5), 892–898.

Vrugt, J. A., Hopmans, J. W. & Šimunek, J. 2001 Calibration of a two-dimensional root water uptake model. *Soil Science Society of America Journal* **65** (4), 1027–1037.

Wang, J. D., Gong, S. H., Sui, J., Xu, H. & Yu, Y. D. 2008 Effects of drip irrigation frequency on the farmland soil water-heat distribution and spring maize growth in North China. *Transactions of the Chinese Society of Agricultural Engineering* **24** (2), 39–45.

Wang, D. L., Feng, H. & Li, Y. 2017 Effects of gravel mulch on soil hydro-thermal process and rain-fed wheat-maize yields. *Transactions of the Chinese Society of Agricultural Engineering* **33** (7), 132–139.

Wang, D., Feng, H., Liu, X., Li, Y., Zhou, L., Zhang, A. & Dyck, M. 2018 Effects of gravel mulching on yield and multilevel water use efficiency of wheat–maize cropping system in semi-arid region of Northwest China. *Field Crops Research* **218**, 201–212.

Xie, Z. K., Wang, Y. J., Wei, X. H. & Zhang, S. H. 2006 Impacts of a gravel–sand mulch and supplemental drip irrigation on watermelon (*Citrullus lanatus* [Thunb.] Mats. & Nakai) root distribution and yield. *Soil and Tillage Research* **89** (1), 35–44.

Yang, J., Mao, X., Wang, K. & Yang, W. 2018 The coupled impact of plastic film mulching and deficit irrigation on soil water/heat transfer and water use efficiency of spring wheat in Northwest China. *Agricultural Water Management* **201**, 232–245.

Yuan, C. P., Lei, T. W., Mao, L. L., Liu, H. & Wu, Y. 2009 Soil surface evaporation processes under mulches of different sized gravel. *Catena* **78** (2), 117–121.

Zhang, Y. L., Feng, S. Y., Wang, F. X. & Binley, A. 2018 Simulation of soil water flow and heat transport in drip irrigated potato field with raised beds and full plastic-film mulch in a semiarid area. *Agricultural Water Management* **209**, 178–187.

Zhang, K., Diao, M., Jing, B., Zhang, X., Wan, W., Guo, P. & Han, W. 2020 Influence of irrigation quota and frequency on root growth and yield of processing tomato. *Journal of Drainage and Irrigation Machinery Engineering* **38** (1), 83–89.

Zhao, W. J., Cui, Z., Zhang, J. Y. & Jin, J. 2017 Temporal stability and variability of soil-water content in a gravel-mulched field in northwestern China. *Journal of Hydrology* **552**, 249–257.

Zhao, Y., Mao, X. M. & Duan, M. 2018a Effects of film mulching and irrigation amount on farmland water–heat dynamics and growth of seed-maize. *Transactions of the Chinese Society for Agricultural Machinery* **49** (8), 275–284.

Zhao, Y., Zhai, X., Wang, Z., Li, H., Jiang, R., Hill, R. L., Si, B. & Hao, F. 2018b Simulation of soil water and heat flow in ridge cultivation with plastic film mulching system on the Chinese Loess Plateau. *Agricultural Water Management* **202**, 99–112.

Zhao, W. J., Cao, T. H., Li, Z. L. & Sheng, J. 2019 Comparison of IDW, cokriging and ARMA for predicting spatiotemporal variability of soil salinity in a gravel–sand mulched jujube orchard. *Environmental Monitoring and Assessment* **191** (6), 376.

Zhao, W. J., Cui, Z. & Zhou, C. Q. 2020 Spatiotemporal variability of soil–water content at different depths in fields mulched with gravel for different planting years. *Journal of Hydrology* **590**, 125253.

First received 9 July 2021; accepted in revised form 4 August 2021. Available online 17 August 2021